Boceprevir, GC-376, and calpain inhibitors II, XII inhibit SARS-CoV-2 viral replication by targeting the viral main protease

Chunlong Ma,[†] Brett Hurst,[‡,§] Yanmei Hu,[†] Tommy Szeto,[†] Bart Tarbet, [‡,§] Jun Wang*, [†]

[†]Department of Pharmacology and Toxicology, College of Pharmacy, The University of Arizona, Tucson, Arizona 85721, United States

[‡]Institute for Antiviral Research, Utah State University, Logan, UT, USA

[§]Department of Animal, Dairy and Veterinary Sciences, Utah State University, Logan, UT, USA

*Corresponding author:

Jun Wang, Tel: 520-626-1366, Fax: 520-626-0749, email: junwang@pharmacy.arizona.edu

Keywords: SARS-CoV-2, COVID-19, main protease, 3CL protease, calpain inhibitors, boceprevir, GC-376

Abstract

A novel coronavirus SARS-CoV-2, also called novel coronavirus 2019 (nCoV-19), started to circulate among humans around December 2019, and it is now widespread as a global pandemic. The disease caused by SARS-CoV-2 virus is called COVID-19, which is highly contagious and has an overall mortality rate of 6.4% as of April 15, 2020. There is no vaccine or antiviral available for SARS-CoV-2. In this study, we report our discovery of inhibitors targeting the SARS-CoV-2 main protease (M^{pro}). Using the FRET-based enzymatic assay, several inhibitors including boceprevir, GC-376, calpain inhibitors II, XII, and MG-132 were identified to have potent activity with single-digit to submicromolar IC_{50} values in the enzymatic assay. The mechanism of action of the hits was further characterized using enzyme kinetic studies and thermal shift binding assays. Significantly, four compounds (boceprevir, GC-376, calpain inhibitors II and XII) inhibit SARS-CoV-2 viral replication in cell culture with EC_{50} values ranging from 0.49 to 3.37 μM. Notably, boceprevir, calpain inhibitors II and XII represent novel chemotypes that are distinct from known M^{pro} inhibitors. Overall, the compounds identified herein provide promising starting points for the further development of SARS-CoV-2 therapeutics.

An emerging respiratory disease COVID-19 started to circulate among human in December 2019. Since its first outbreak in China from an unknown origin, it quickly became a global pandemic. As of April 15, 2020, there are 123,010 deaths among 1,914,916 confirmed cases in 213 countries.[1] The etiological pathogen of COVID-19 is a new coronavirus, the severe acute respiratory syndrome coronavirus 2 (SARS-CoV-2), also called novel coronavirus (nCoV-2019). As the name indicates, SARS-CoV-2 is similar to SARS, the virus that causes severe respiratory symptoms in human and killed 774 people among 8098 infected worldwide in 2003.[2] SARS-CoV-2 shares ~82% of sequence identity as SARS and to a less extent for Middle East respiratory syndrome (MERS) (~50%).[3,4] SARS-CoV-2 is an enveloped, positive-sense, single-stranded RNA virus that belongs to the β-lineage of the coronavirus.[5] The β-lineage also contains two other important human pathogens, the SARS coronavirus and MERS coronavirus. The mortality rate of SARS-CoV-2 is around 6.4% as of April 15, 2020, which is lower than that of SARS (~10%) and MERS (~34%).[2] However, current data indicate that SARS-CoV-2 is more contagious and has a larger R0 value than SARS and MERS,[6] resulting in higher overall death tolls than SARS and MERS. The SARS-CoV-2 virus is currently spreading at an alarming speed in Europe and the United States.

There is currently no antiviral or vaccine for SARS-CoV-2. The SARS-CoV-2 viral genome encodes a number of structural proteins (e.g. capsid spike glycoprotein), non-structural proteins (e.g. 3-chymotrypsin-like protease (3CL or main protease), papain-like protease, helicase, and RNA-dependent RNA polymerase), and accessary proteins. Compounds that target anyone of these viral proteins might be potential antiviral drug candidates. In this study, we focus on the viral 3CL protease, also called the main protease (M^{pro}), and aim to develop potent M^{pro} inhibitors as SAR-CoV-2 antivirals. The M^{pro} plays an essential role in coronavirus replication

by digesting the viral polyproteins at more than 11 sites, and it appears like a high profile target for antiviral drug discovery.[7-9] The M^{pro} has an unique substrate preference for glutamine at the P1 site (Leu-Gln↓(Ser,Ala,Gly)), a feature that is absent in closely related host proteases, suggesting it is feasible to achieve high selectivity by targeting viral M^{pro}. As such, we developed the Fluorescence Resonance Energy Transfer (FRET)-based enzymatic assay for the SARS-CoV-2 M^{pro} and applied it to screen a focused library of protease inhibitors. Here we report our findings of several hits targeting SARS-CoV-2 M^{pro} and their mechanism of action. The in vitro antiviral activity of the hits was also evaluated in cell culture using infectious SARS-CoV-2 virus. Overall, our study provides a list of drug candidates for SARS-CoV-2 with a confirmed mechanism of action, and the results might help speed up the drug discovery efforts in combating COVID-19. The compounds identified herein represent the most potent and selective SARS-CoV-2 M^{pro} inhibitors so far with both enzymatic inhibition and cellular antiviral activity.[7,9]

Results

Establishing the FRET-based assay for the SARS-CoV-2 main protease (M^{pro})

The M^{pro} gene from SARS-CoV-2 strain BetaCoV/Wuhan/WIV04/2019 was inserted into pET-29a(+) vector and expressed in BL21(DE3) *E. Coli.* with a His-tag in its C-terminus. The M^{pro} protein was purified with Ni-NTA column to high purity (Fig. 1A). To establish the FRET assay condition, we designed a FRET based substrate using the sequence between viral polypeptide NSP4-NSP5 junction from SARS-CoV-2: Dabcyl-KTSAVLQ/SGFRKME(Edans). We then tested the M^{pro} proteolytic activity in buffers with different pH. We found that M^{pro} displays highest activity in pH 6.5 buffer (Fig. 1B), which contains 20 mM HEPES, 120 mM NaCl, 0.4 mM EDTA,

and 4 mM DTT and 20% glycerol. As such, all the following proteolytic assay was conducted using this pH 6.5 buffer. Next, we characterized the enzymatic activity of this SARS-CoV-2 M^{pro} by measuring the K_m and V_{max} values. When 100 nM M^{pro} was mixed with various concentration of FRET substrate (0 to 200 µM), the initial velocity was measured and plotted against substrate concentration. Curve fitting with Michaelis-Menton equation gave the best-fit values of K_m and V_{max} as 32.8 ± 3.5 µM and 29.4 ± 1.1 RFU/s, respectively (Fig. 1C).

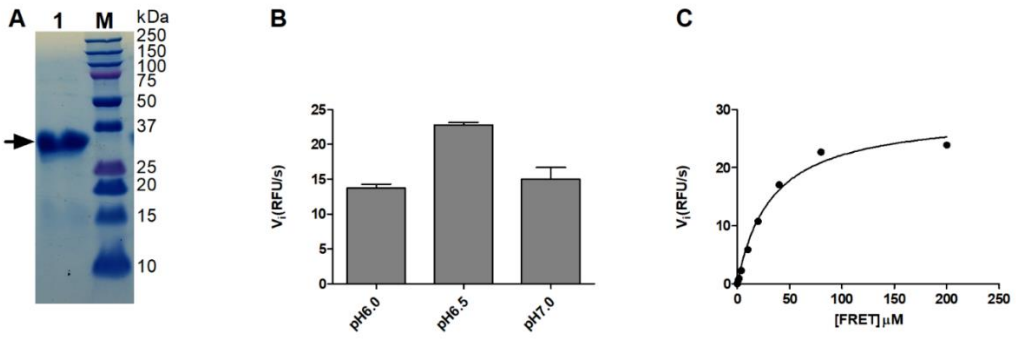

Figure 1: SARS-CoV-2 M^{pro} expression and characterization. (A) SDS-PAGE of His-tagged-Main protease (M^{pro}) (lane 1); Lane M, protein ladder; the calculated molecular weight of the His-tagged-M^{pro} is 34,992 Da. (B) Reaction buffer optimization: 250 nM His-tagged-M^{pro} was diluted into three reaction buffers with different pH values. (C) Michaelis-Menten plot of 100 nM His-tagged- M^{pro} with the various concentrations of FRET substrate in pH 6.5 reaction buffer.

Primary screening of a focused protease library against the SARS-CoV-2 M^{pro}.

With the established FRET assay condition, we screened a collection of protease inhibitors from the Selleckchem bioactive compound library to identify potential SARS-CoV-2 M^{pro} inhibitors.

The protease inhibitors are grouped based on their targets and mechanism of action and include proteasome inhibitors (**1-8**); HIV protease inhibitors (**9-14**); γ-secretase inhibitors (**15-22**); HCV NS3-4A protease inhibitors (**23-29**); DPP-4 inhibitors (**30-35**); miscellaneous serine protease inhibitors (**36-39**); cathepsin and calpain protease inhibitors (**40-43**); miscellaneous cysteine protease inhibitors (**44-48**); matrix metalloprotease inhibitors (**49-51**); and miscellaneous protease inhibitors (**52-55**). The inhibitors were pre-incubated with 100 nM of M^{pro} at 30 °C for 30 minutes in the presence of 4 mM 1,4-dithiothreitol (DTT) before the addition of 10 µM FRET substrate. The addition of DTT was to quench non-specific thiol reactive compounds and also to ensure the M^{pro} is in the reducing condition. All compounds were tested at 20 µM, except compound **26**, which was tested at 2 µM due to its fluorescent background. Encouragingly, four inhibitors (**24**, **28**, **29** and **43**) showed more than 60% inhibition against M^{pro} at 20 µM. Among the hits, simeprevir (**24**), boceprevir (**28**), and narlaprevir (**29**) are HCV NS3-4A serine protease inhibitors, and compound MG-132 (**43**) inhibits both proteasome and calpain.

Table 1. List of protease inhibitors tested against SARS-CoV-2 M^{pro} in the primary FRET assay.

Proteosome inhibitors

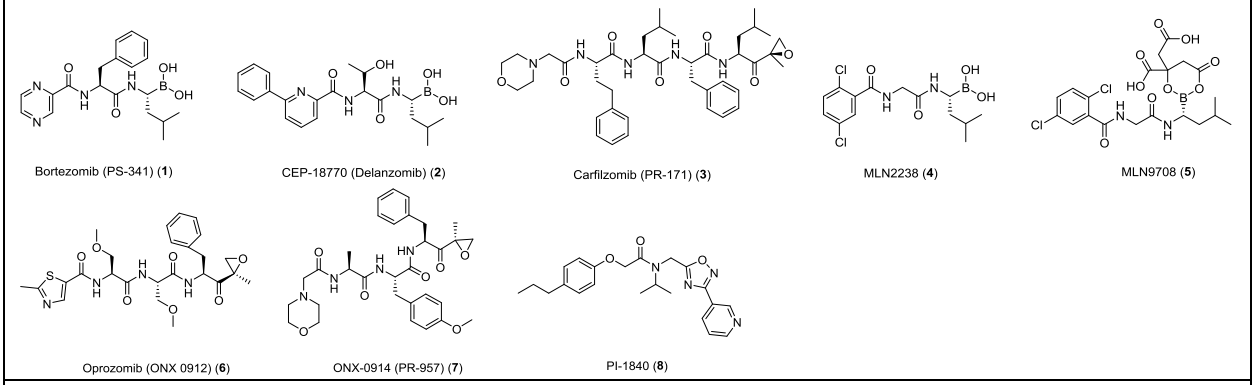

HIV protease (aspartic protease) inhibitors

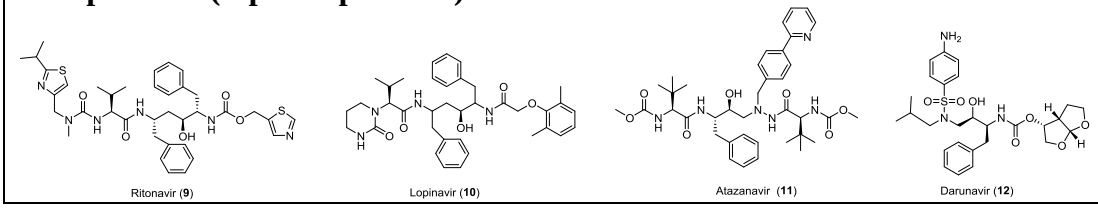

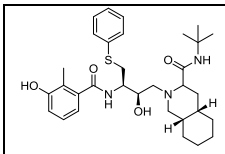

Nelfinavir (**13**)

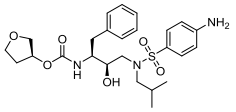

Amprenavir (**14**)

γ-secretase (aspartic protease) inhibitors

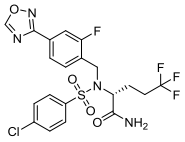

Avagacestat (**15**)

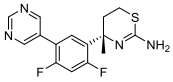

LY2811376 (**16**)

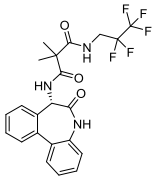

RO4929097 (**17**)

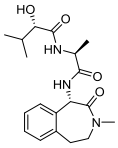

Semagacestat (LY450139) (**18**)

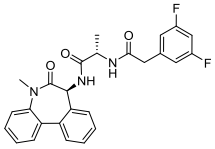

YO-01027 (**19**)

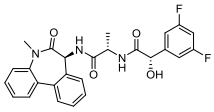

LY411575 (**20**)

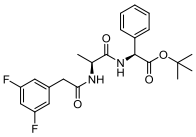

DAPT (GSI-IX) (**21**)

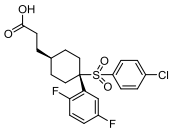

MK-0752 (**22**)

HCV protease (serine protease) inhibitors

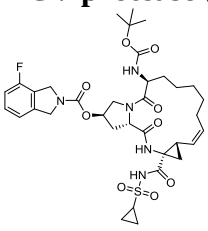

Danoprevir (**23**)

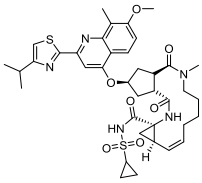

Simeprevir (**24**)

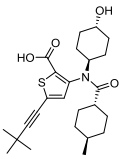

Lomibuvir (VX-222) (**25**)

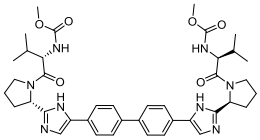

Daclatasvir (BMS-790052) (**26**)

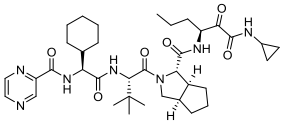

Telaprevir (**27**)

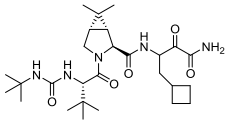

Boceprevir (**28**)

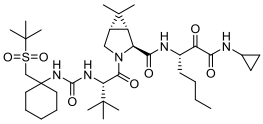

Narlaprevir (**29**)

DPP-4 (serine protease) inhibitors

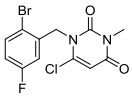

Trelagliptin (**30**)

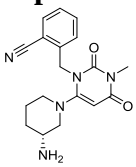

Alogliptin (**31**)

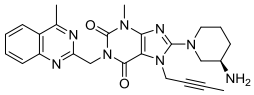

Linagliptin (**32**)

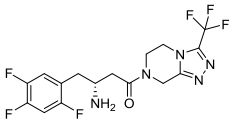

Sitagliptin (**33**)

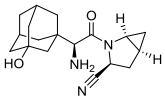

Saxagliptin (**34**)

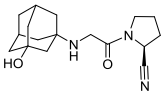

Vildagliptin (**35**)

Miscellaneous serine protease inhibitors

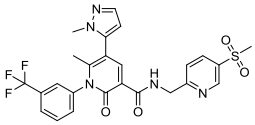

Alvelestat (**36**)

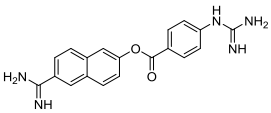

Nafamostat Mesylate (**37**)

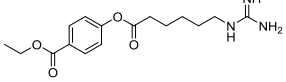

Gabexate (**38**)

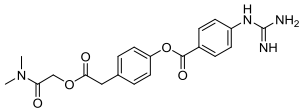

Camostat Mesilate (**39**)

Cathepsin and calpain protease (cysteine protease) inhibitors

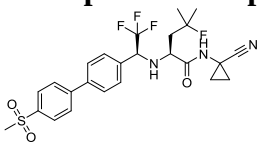

Odanacatib (MK-0822) (**40**)

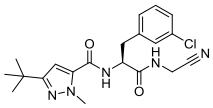

Cathepsin Inhibitor 1 (**41**)

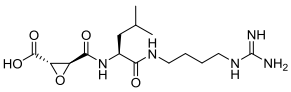

E-64 (**42**)

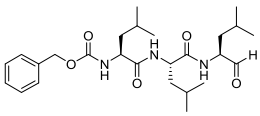

MG-132 (**43**)

Miscellaneous cysteine protease inhibitors

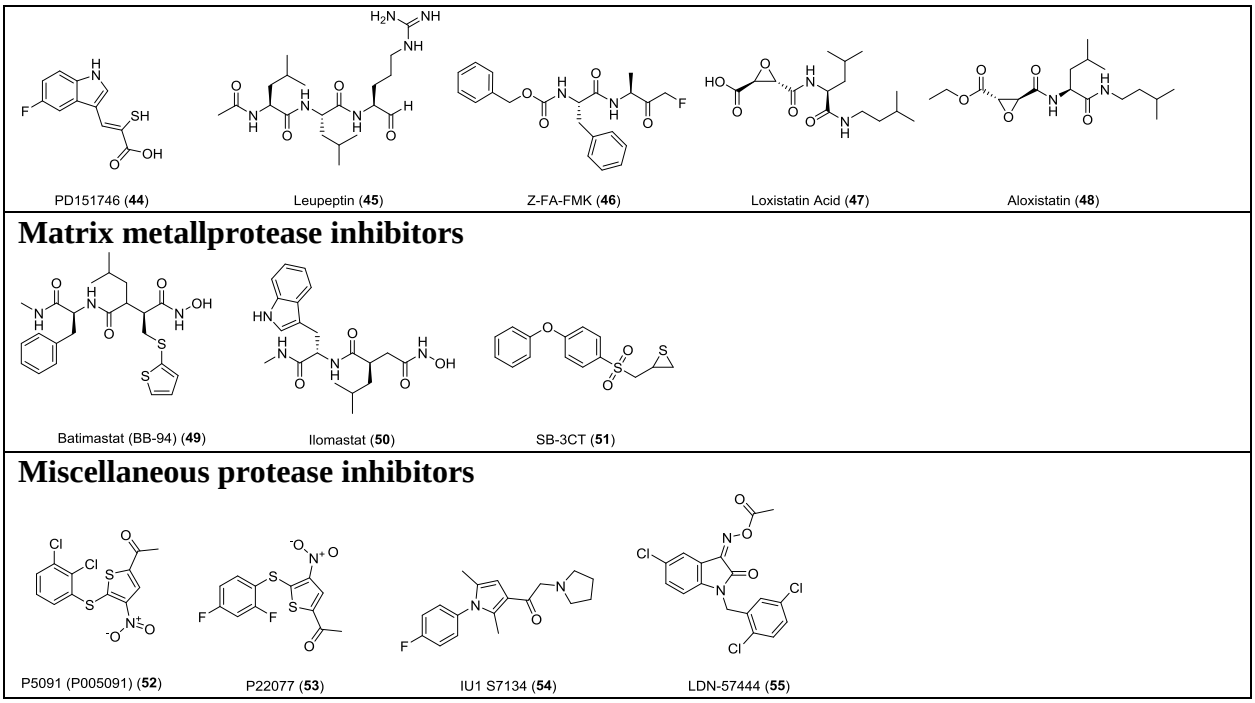

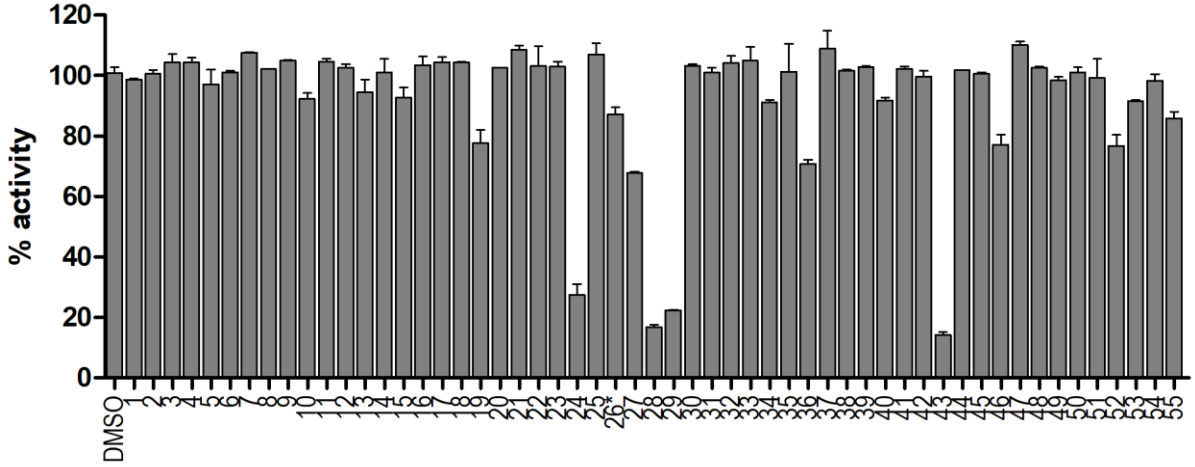

Figure 2: Screening of known protease inhibitors against SARS-CoV-2 M^{pro} using the FRET assay. 20 µM of compounds (**26** was tested at 2 µM) was pre-incubated with 100 nM of SARS-CoV-2 M^{pro} for 30 minutes at 30 °C, then 10 µM FRET substrate was added to reaction mixture to initiate the reaction. The reaction was monitored for 2 hours. The initial velocity was calculated by linear regression using the data points from the first 15 minutes of the reaction. The

calculated initial velocity with each compound was normalized to DMSO control. The results are average ± standard deviation of two repeats.

Secondary screening of a focused library of calpain/cathepsin inhibitors and known viral 3CL^{pro} inhibitors

Given the encouraging results from the primary screening, we then further characterized the four hits (**24**, **28**, **29**, and **43**) in a consortium of assays including dose-response titration, thermal shift binding assay (TSA), and counter screening assays with two other viral cysteine proteases, the enterovirus A71 (EV-A71) 2A and 3C proteases, both of which are cysteine proteases. The HCV NS3-4A protease inhibitors boceprevir (**28**) and narlaprevir (**29**) inhibited M^{pro} with IC_{50} values of 4.13 and 4.73 μM, respectively (Table 2), more potent than simeprevir (**24**) (IC_{50} = 13.74 μM). Both compounds **28** and **29** also showed strong binding towards M^{pro} and shifted the melting temperature of the protein (ΔT_m) by 6.67 and 5.18 ^oC, respectively, at 40 μM. Despite their potent inhibition against the HCV NS3-4A serine protease and the SARS-CoV-2 cysteine M^{pro}, boceprevir (**28**) and narlaprevir (**29**) did not inhibit the EV-A71 2A and 3C proteases (IC_{50} > 20 μM), suggesting they are not non-specific cysteine protease inhibitors. The calpain inhibitor MG-132 (**43**) had an IC_{50} value of 3.90 μM against the M^{pro}, and was not active against the EV-A71 2A and 3C proteases (IC_{50} > 20 μM). The binding of MG-132 (**43**) to M^{pro} was also confirmed in the TSA assay with a ΔT_m of 4.02 ^oC.

In light of the promising results of the calpain inhibitor MG-132 (**43**), we then pursued to testing other calpain and cathepsin inhibitors that are commercially available (**56**-**63**) (Table 2). These compounds were not included in the initial library because they have not been advanced to clinical studies. Among this series of analogs, calpain inhibitor II (**61**) and XII (**62**) are the most potent

M^{pro} inhibitors with IC_{50} values of 0.97 and 0.45 μM, respectively. Binding of compounds **61** and **62** to M^{pro} shifted the melting curve of the protein by 6.65 and 7.86 ^{o}C, respectively. Encouragingly, both compounds **61** and **62** did not inhibit the EV-A71 2A and 3C proteases (IC_{50} > 20 μM). Calpain inhibitor I (**59**) and MG-115 (**60**) also showed potent inhibition against M^{pro} with IC_{50} values of 8.60 and 3.14 μM, respectively. Calpeptin (**56**) and PSI (**63**) had moderate activity against M^{pro} with IC_{50} values of 10.69 and 10.38 μM, respectively. In contrast, calpain inhibitors III (**57**) and VI (**58**) were not active (IC_{50} > 20 μM).

We also included two well-known viral 3CL protease inhibitors GC-376 (**64**) and rupintrivir (**65**) in the secondary screening. GC-376 (**64**) is an investigational veterinary drug that is being developed for feline infectious peritonitis (FIP).[10,11] GC-376 (**64**) was designed to target the viral 3CL protease and had potent antiviral activity against multiple viruses including MERS, FIPV, and norovirus.[10,12] Rupintrivir (**65**) was developed as a rhinovirus antiviral by targeting the viral 3CL protease, but it was discontinued in clinical trials due to side effects.[13] In our study, we found that GC-376 (**64**) was the most potent M^{pro} inhibitor with an IC_{50} value of 0.03 μM. It shifted the melting curve of M^{pro} by 18.30 ^{o}C upon binding. In contrast, rupintrivir (**65**) was not active against M^{pro} (IC_{50} > 20 μM). Previous report also showed that rupintrivir was not active against the SARS-CoV $3CL^{pro}$ (M^{pro}) (IC_{50} > 100 μM).[14] Both compounds **64** and **65** were not active against the EV-A71 2A protease, but showed potent inhibition against the EV-A71 3C protease, which is consistent with previously reported results.[12,15,16]

Table 2: Characterization of HCV and calpain proteases inhibitors against SARS-CoV-2 M^{pro} using a consortium of secondary assays[a]

ID / Results	SARS-CoV-2 M^{pro} IC_{50} (μM)	2019-nCoV 3CL TSA Tm/ΔTm (°C)	EV-A71 2A IC_{50} (μM)	EV-A71 3C IC_{50} (μM)	Development stage

DMSO	-------	55.74 ± 0.00	------	-------	
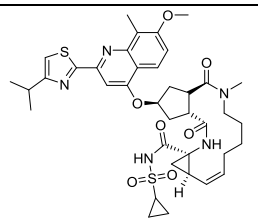 Simeprevir (**24**)	13.74 ± 3.45	N.T.[b]	N.T.	N.T.	FDA-approved HCV drug
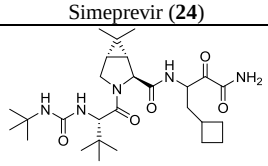 Boceprevir (**28**)	4.13 ± 0.61	62.41 ± 0.21/6.67	>20	>20	FDA-approved HCV drug
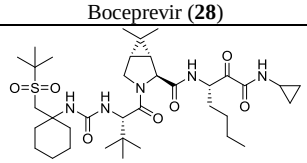 Narlaprevir (**29**)	5.73 ± 0.67	60.92 ± 0.14/5.18	>20	>20	FDA-approved HCV drug
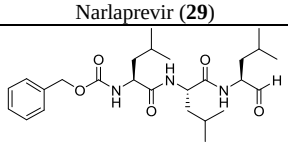 MG-132 (ApexBio) (**43**)	3.90 ± 1.01	59.76 ± 0.45/4.02	>20	>20	Preclinical; tested in mice[17]
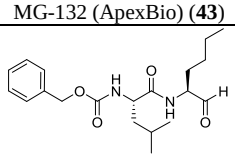 Calpeptin (**56**)	10.69 ± 2.77	56.84 ± 0.00/1.1	>20	>20	Preclinical; tested in mice and feline[18,19]
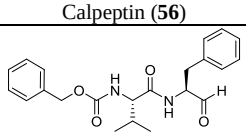 calpain inhibitor III (MDL28170) (**57**)	>20	55.36 ± 0.14/-0.38	N.T.	N.T.	Preclinical; not tested in animal model
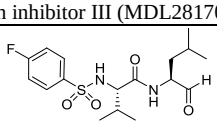 Calpain inhibitor VI (**58**)	>20	55.46 ± 0.14/-0.28	N.T.	>20	Preclinical; tested in rats[20]
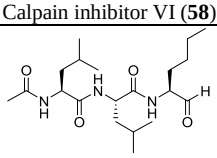 Calpain inhibitor I (ALLN) (**59**)	8.60 ± 1.46	N.T.	>20	>20	Preclinical; tested in mice[21]
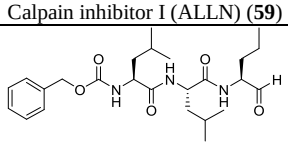 MG-115 (**60**)	3.14 ± 0.97	60.51 ± 0.28/4.77	>20	>20	Preclinical; not tested in animal model
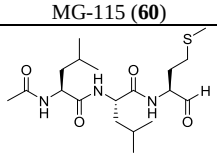 Calpain inhibitor II (ALLM) (**61**)	0.97 ± 0.27	62.93 ± 0.14/6.65	>20	>20	Preclinical; not tested in animal model

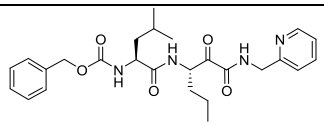 Calpain inhibitor XII (**62**)	0.45 ± 0.06	63.60 ± 0.01/7.86	>20	>20	Preclinical; not tested in animal model
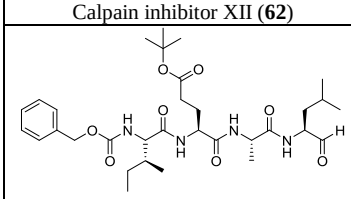 PSI (**63**)	10.38 ± 2.90[c]	N.T.	1.22	13.74 ± 3.86	Preclinical; tested in rats[22]
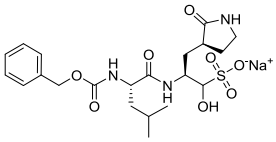 GC376 (more reliable) (**64**)	0.030 ± 0.008	74.04 ± 0.07/18.30	>20	0.136 ± 0.025	Preclinical; tested in feline[10,11]
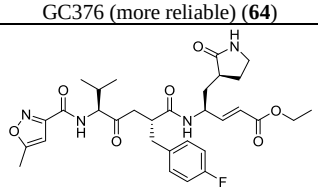 Rupintrivir (**65**)	> 20	N.T.	>20	0.042 ± 0.014	Dropped out of clinical trial

a: Value = mean ± S.E. from 2 to 3 independent experiments;

b: N.T. = not tested;

c: The IC_{50} of PSI (**64**) on SARS CoV-2 M^{pro} was calculated by end point reading of 1 hour digestion, instead of the initial velocity.

When plotting the IC_{50} values (log scale) of the inhibitors against M^{pro} from the FRET enzymatic assay with the melting temperature shifts (ΔT_m) from thermal shift binding assay (Fig. 3A), a linear correlation was observed, and the r^2 of the linear regression fitting is 0.94. This suggests that there is a direct correlation between the enzymatic inhibition and protein binding: a more potent enzyme inhibitor also binds to the protein with higher affinity. The stabilization of the M^{pro} against thermal denaturation was also compound concentration dependent (Fig. 3B).

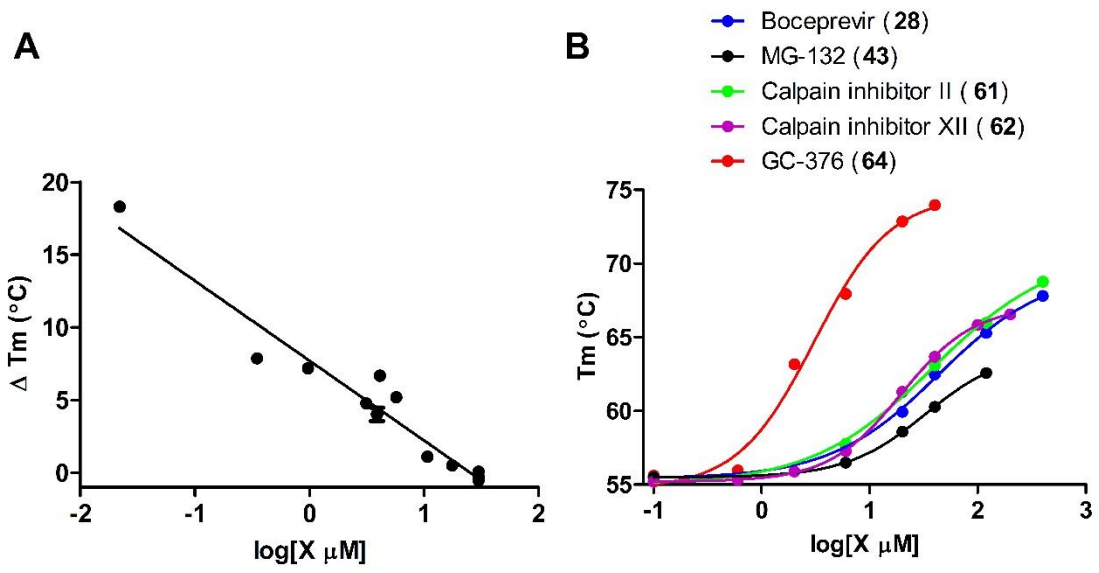

Figure 3: Binding of inhibitors to SARS-CoV-2 M^{pro} using thermal shift binding assay. (A) Correlation of inhibition efficacy (IC_{50}) with ΔT_m from thermal shift binding assay. Data in Table 2 were used for the plot. The r^2 of fitting is 0.94. (B) Dose-dependent melting temperature (T_m) shift.

Mechanism of action of hits

To elucidate the mechanism of action of hits against SARS-CoV-2 M^{pro}, we focus on five most potent compounds prioritized from the primary and secondary screenings including boceprevir (**28**), MG-132 (**43**), calpain inhibitor II (**61**), calpain inhibitor XII (**62**), and GC-376 (**64**). For this, we performed enzyme kinetic studies with different concentrations of inhibitors (Fig. 4). A biphasic enzymatic progression curve in the presence but not in the absence of inhibitor is typically a hallmark for a slow covalent binding inhibitor. In the Fig. 4, left column shows the progression curves up to 4 hours. Biphasic progression curves were observed for all 5 inhibitors at high drug concentrations. Significant substrate depletion was observed when the proteolytic reaction

proceeded beyond 90 minutes, we therefore chose the first 90 minutes of the progression curves for curve fitting (Fig. 4 middle column). We fit the progression curves in the presence different concentrations of GC-376 (**64**) with the two-step Morrison equation (equation 3 in methods section). GC-376 (**64**) binds to SARS-CoV-2 M^{pro} with an equilibrium dissociation constant for the inhibitor (K_I) of 59.9 ± 21.7 nM in the first step. After initial binding, a slower covalent bond is formed between GC-376 (**64**) and M^{pro} with the second reaction rate constant (k_2) being 0.00245 ± 0.00047 s^{-1}, resulting an overall k_2/K_I value of 4.08 x 10^4 M^{-1} s^{-1} (Fig. 4A). However, when we tried to fit the proteolytic progression curves for boceprevir (**28**), MG-132 (**43**), calpain inhibitors II (**61**) and XII (**62**) using the same two-step reaction mechanism, we could not obtain accurate values for the second rate constant k_2. This is presumably due to significant substrate depletion before the equilibrium between EI and EI*, leading to very small values of k_2. Accordingly, for these four inhibitors **28**, **43**, **61**, and **62**, only the dissociation constant K_I values from the first step were determined (Figs. 6B-6E). The inhibition constants (K_I) for boceprevir (**28**), MG-132 (**43**), calpain inhibitors II (**61**) and XII (**62**) are 1.18 ± 0.10 μM, 1.57 ± 0.13 μM, 0.40 ± 0.02 μM, and 0.13 ± 0.02 μM, respectively.

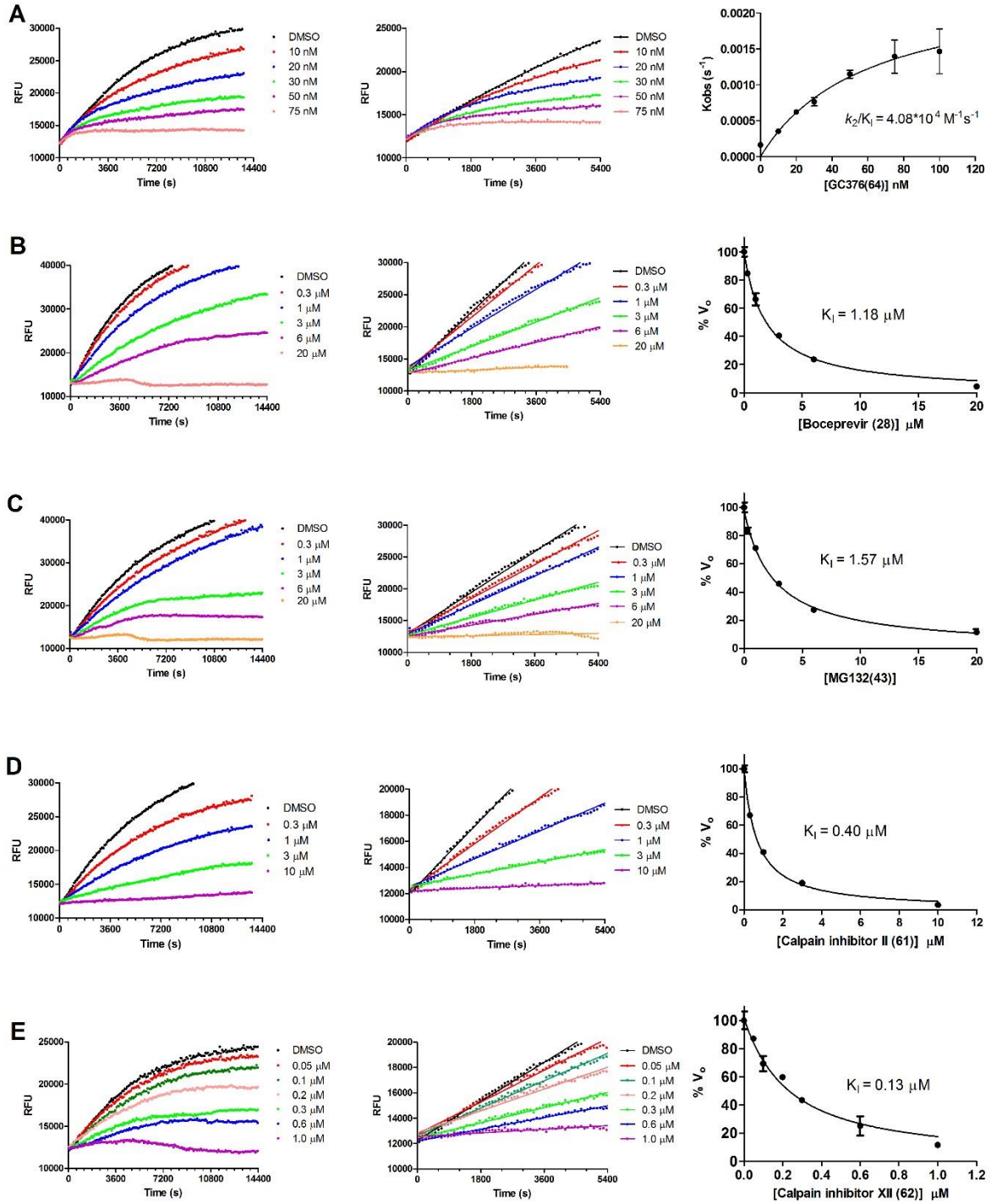

Figure 4: Proteolytic reaction progression curves of M^{pro} in the presence or the absence of compounds. In the kinetic studies, 5 nM M^{pro} was added to a solution containing various concentrations of protease inhibitors and 20 μM FRET substrate to initiate the reaction, the

reaction was then monitored for 4 hrs. Left column shows the reaction progression up to 4 hrs; middle column shows the progression curves for the first 90 minutes, which were used for curve fitting to generate the plot shown in the right column. Detailed methods were described in the Method section. (A) GC-376 (**64**); (B) Boceprevir (**28**); (C) MG-132 (**43**); (D) Calpian inhibitor II (**61**); (E) Calpain inhibitor XII (**62**).

Cellular antiviral activity and cytotoxicity of hits

To test the hypothesis that inhibiting the enzymatic activity of M^{pro} will lead to the inhibition of SARS-CoV-2 viral replication, we performed cellular antiviral assays for the five promising hits **64**, **28**, **43**, **61**, and **62** against SARS-CoV-2. For this, we first tested the cellular cytotoxicity of these compounds in multiple cell lines (Table 3). GC-376 (**64**), boceprevir (**28**), and calpain inhibitor II (**61**) were well tolerated and had CC_{50} values of over 100 μM for all the cell lines tested. MG-132 (**43**) was cytotoxic to all the cells with CC_{50} values less than 1 μM except A549 cells. Calpain inhibitor XII (**62**) had acceptable cellular cytotoxicity with CC_{50} values above 50 μM for all the cell lines tested.

Table 3: Selected protease inhibitors cytotoxicity on various cell lines[a]

	GC-376 (**64**)	Boceprevir (**28**)	MG-132 (**43**)	Calpain inhibitor II (**61**)	Calpain inhibitor XII (**62**)
MDCK	>100	>100	0.34 ± 0.02	>100	60.36 ± 2.28
Vero	>100	>100	0.45 ± 0.02	>100	>100
HCT-8	>100	>100	0.47 ± 0.02	>100	73.29 ± 11.80
A549	>100	>100	10.71 ± 3.50	>100	>100
Caco-2	>100	>100	<0.15	>100	82.02 ± 0.37
BEAS2B	>100	>100	0.14 ± 0.03	>100	78.91 ± 13.70

a: Cytotoxicity was evaluated by measuring CC_{50} values (50% cytotoxic concentration) with CPE assay described in the method section. CC_{50} = mean ± S.E. of 2 or 3 independent experiments.

Next, we chose four compounds boceprevir (**28**), calpain inhibitors II (**61**), XII (**62**), and GC-376 (**64**) for the antiviral assay with infectious SARS-CoV-2. MG-132 (**43**) was not included due to its cytotoxicity. Gratifyingly, all four compounds showed potent antiviral activity against SARS-CoV-2 in the primary viral cytopathic effect (CPE) assay with EC_{50} values ranging from 0.49 to 3.37 μM (Table 4). Their antiviral activity was further confirmed in the secondary viral yield reduction (VYR) assay. The most potent compound was calpain inhibitor XII (**62**), which showed EC_{50} of 0.49 μM in the primary CPE assay and EC_{90} of 0.45 μM in the secondary VYR assay. In comparison, remdesivir was reported to inhibit SARS-CoV-2 in the VYR assay with an EC_{50} of 0.77 μM.[23] None of the compounds inhibited the unrelated influenza virus A/California/07/2009 (H1N1) virus (EC_{50} > 20 μM), suggesting the antiviral activity of the four compounds (boceprevir, calpain inhibitors II, XII, and GC-376) against SARS-CoV-2 is specific.

Table 4: Antiviral activity of hits against SARS-CoV-2 in CPE assay

Compounds	SARS-CoV-2 Antiviral activity (μM) Primary CPE assay[a]	SARS-CoV-2 Antiviral activity (μM) Secondary viral yield reduction assay[a]	A/California/07/2009 (H1N1) antiviral activity (μM)[a]
Boceprevir (**28**)	EC_{50} = 1.90 CC_{50} > 100 SI_{50} > 52.6	N.T.	> 20
Calpain inhibitor II (**61**)	EC_{50} = 2.07 ± 0.76 CC_{50} > 100 SI_{50} > 48.3	EC_{90} = 2.40 ± 1.01	> 20
Calpain inhibitor XII (**62**)	EC_{50} = 0.49 ± 0.18 CC_{50} > 100 SI_{50} > 204	EC_{90} = 0.45 ± 0.17	> 20
GC-376 (**64**)	EC_{50} = 3.37 ± 1.68 CC_{50} > 100 SI_{50} > 29.7	EC_{90} = 2.13 ± 1.05	> 20

[a]CPE EC_{50}, VYR EC_{90}, and cytotoxicity CC_{50} values are mean ± S.D. of 3 independent experiments.

Discussion

Coronaviruses have caused three epidemics/pandemics in the past twenty years including SARS, MERS, and COVID-19. With the ongoing pandemic of COVID-19, scientists and researchers around the globe are racing to find effective vaccines and antiviral drugs.[24] The viral polymerase inhibitor remdesivir holds the greatest promise and it is currently being evaluated in several clinical trials.[25,26] The HIV drug combination lopinavir and ritonavir recently failed in a clinical trial for COVID-19 with no significant therapeutic efficacy was observed.[27] To address this unmet medical need, we initiated a drug repurposing screening to identify potent inhibitors against the SARS-CoV-2 M^{pro} from a collection of FDA-approved protease inhibitors. The M^{pro} has been shown to be a validated antiviral drug target for SARS and MERS.[28] As the SARS-CoV-2 M^{pro} shares a high sequence similarity with SARS and to a less extent with MERS, we reasoned that inhibiting the enzymatic activity of SARS-CoV-2 M^{pro} will similarly prevent viral replication.[7,9] Noticeable findings from our study include: 1) Boceprevir (**28**), an FDA-approved HCV drug, inhibits the enzymatic activity of M^{pro} with IC_{50} of 4.13 μM, and has an EC_{50} of 1.90 μM against the SARS-CoV-2 virus in the cellular viral cytopathic effect assay. The therapeutic potential of boceprevir (**28**) should be further evaluated in relevant animal models and human clinic trials. Since boceprevir (**28**) is a FDA-approved drug, the dose, toxicity, formulation, and pharmacokinetic properties are already known, which will greatly speed up the design of follow up studies; 2) GC-376 (**64**), an investigational veterinary drug, showed promising antiviral activity against the SARS-CoV-2 virus (EC_{50} = 3.37 μM). It has the highest enzymatic inhibition against the M^{pro} with an IC_{50} value of 0.03 μM. This compound has promising in vivo

efficacy in treating cats infected with FIP, and has favorable in vivo pharmacokinetic properties. Therefore, GC-376 (**64**) is ready to be tested in relevant animal models of SARS-CoV-2 when available; 3) Three calpain/cathepsin inhibitors, MG-132 (**43**), calpain inhibitors II (**61**) and XII (**62**), are potent inhibitors of M^{pro} and inhibit SARS-CoV-2 with single-digit to submicromolar efficacy in the enzymatic assay. Calpain inhibitors II (**61**) and XII (**62**) also inhibit SARS-CoV-2 in the CPE assay with EC_{50} values of 2.07 and 0.49 μM, respectively. This result suggests that calpain/cathepsin inhibitors are rich sources of drug candidates for SARS-CoV-2. A significant number of calpain/cathepsin inhibitors have been developed over the years for various diseases including cancer, neurodegeneration disease, kidney diseases, and ischemia/reperfusion injury.[29] Given the promising results of calpain inhibitors II (**61**) and XII (**62**) in inhibiting the SARS-CoV-2 M^{pro} and their potent antiviral activity in cell culture, it might be worthwhile to repurposing them as antivirals for SARS-CoV-2.

All potent SARS-CoV-2 M^{pro} inhibitors contain reactive warheads such as α-ketoamide (boceprevir (**28**), calpain inhibitor XII (**62**)) or aldehyde (MG-132 (**43**), calpain inhibitor II (**61**)) or aldehyde prodrug, the bisulfite (GC-376 (**64**)). This result suggests that reactive warheads might be essential for SARS-CoV-2 M^{pro} inhibition. The compounds identified in this study represent the most potent and selective hits reported so far, and are superior than recently reported SARS-CoV-2 M^{pro} inhibitors **ebselen**, **N3**, and **13b** (Table 5).

Table 5: Literature reported SARS-CoV-2 M^{pro} inhibitors.

	SARS-CoV-2 M^{pro} inhibition	SARS-CoV-2 Antiviral EC_{50} (μM)	Development Stage
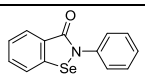 **Ebselen**[9]	IC_{50} = 0.67 ± 0.09 μM	4.67 ± 0.80	In clinical trials

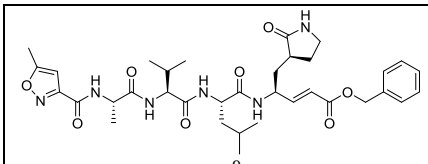 **N3**[9]	k_{obs}/[I] = 11,300 ± 800 $M^{-1}S^{-1}$	16.77 ± 1.70	Preclinical;[30] not tested in animal model
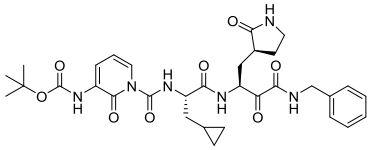 **13b**[7]	IC_{50} = 0.67 ± 0.18 μM	4 ~ 5	Preclinical;[7] not tested in animal model

Results in the table were retrived from recent publications.[7,9]

Aside from the above positive results, we also showed that ritonavir (**9**) and lopinavir (**10**) failed to inhibit the SARS-CoV-2 M^{pro} (IC_{50} > 20 μM, Fig. 2), which might explain their lack efficacy in clinical trials for COVID-19.[27] Camostat (**39**) was recently proposed to inhibit SARS-CoV-2 entry through inhibiting the host TMPRSS2, a host serine protease that is important for viral S protein priming.[31] However, the antiviral activity of camostat has not been confirmed with infectious SARS-CoV-2 virus. In our study, we found camostat (**39**) has no inhibition against the SARS-CoV-2 M^{pro} (IC_{50} > 20 μM).

In summary, this study identified several potent SARS-CoV-2 M^{pro} inhibitors with potent enzymatic inhibition as well as potent cellular antiviral activity. Further development based on these hits might lead to clinically useful COVID-19 antivirals. They can be used either alone or in combination with polymerase inhibitors such as remdesivir as a means to achieve potential synergic antiviral effect as well as to suppress drug resistance.

Methods

Cell lines and viruses. Human rhabdomyosarcoma (RD); A549, MDCK, Caco-2, and Vero cells were maintained in Dulbecco's modified Eagle's medium (DMEM), BEAS2B and HCT-8 cells

were maintained in RPMI 1640 medium. Both medium was supplemented with 10% fetal bovine serum (FBS) and 1% penicillin-streptomycin antibiotics. Cells were kept at 37°C in a 5% CO2 atmosphere. The USA_WA1/2020 strain of SARS-CoV-2 obtained from the World Reference Center for Emerging Viruses and Arboviruses (WRCEVA).

Protein expression and purification. SARS CoV-2 main protease (M^{pro} or 3CL) gene from strain BetaCoV/Wuhan/WIV04/2019 was ordered from GenScript (Piscataway, NJ) in the pET29a(+) vector with E. coli codon optimization. pET29a(+) plasmids with SARS CoV-2 main protease was transformed into competent E. coli BL21(DE3) cells, and a single colony was picked and used to inoculate 10 ml of LB supplemented with 50 g/ml kanamycin at 37°C and 250 rpm. The 10-ml inoculum was added to 1 liter of LB with 50 g/ml kanamycin and grown to an optical density at 600 nm of 0.8, then induced using 1.0 mM IPTG. Induced cultures were incubated at 37 °C for an additional 3 h and then harvested, resuspended in lysis buffer (25 mM Tris [pH 7.5], 750 mM NaCl, 2 mM dithiothreitol [DTT] with 0.5 mg/ml lysozyme, 0.5 mM phenylmethylsulfonyl fluoride [PMSF], 0.02 mg/ml DNase I), and lysed with alternating sonication and French press cycles. The cell debris were removed by centrifugation at 12,000 g for 45 min (20% amplitude, 1 s on/1 s off). The supernatant was incubated with Ni-NTA resin for over 2 h at 4°C on a rotator. The Ni-NTA resin was thoroughly washed with 30 mM imidazole in wash buffer (50 mM Tris [pH 7.0], 150 mM NaCl, 2 mM DTT); and eluted with 100 mM imidazole in 50 mM Tris [pH 7.0], 150 mM NaCl, 2 mM DTT. The imidazole was removed via dialysis or on a 10,000-molecular-weight-cutoff centrifugal concentrator spin column. The purity of the protein was confirmed with SDS-PAGE. The protein concentration was determined via 260nM absorbance with ε 32890. EV-A71 2Apro and 3Cpro were expressed in the pET28b(+) vector as previously described [15,32,33].

Peptide synthesis. The SARS-CoV-2 M^{pro} FRET substrate Dabcyl-KTSAVLQ/SGFRKME(Edans) was synthesized by solid-phase synthesis through iterative cycles of coupling and deprotection using the previously optimized procedure.[34] Specifically, chemmatrix rink-amide resin was used. Typical coupling condition was 5 equiv of amino acid, 5 equiv of HATU, and 10 equiv of DIEA in DMF for 5 minutes at 80 ^{o}C. For deprotection, 5% piperazine plus 0.1 M HOBt were used and the mixture was heated at 80°C for 5 minutes. The peptide was cleaved from the resin using 95% TFA, 2.5% Tris, 2.5% H_2O and the crude peptide was precipitated from ether after removal of TFA. The final peptide was purified by preparative HPLC. The purify and identify of the peptide were confirmed by analytical HPLC (> 98% purity) and mass spectrometry. $[M+3]^{3+}$ calculated 694.15, detected 694.90; $[M+4]^{4+}$ calculated 520.86, detected 521.35;

Enzymatic assays. For reaction condition optimization, 200 µM SARS CoV-2 Main protease was used. pH6.0 buffer contains 20 mM MES pH6.0, 120 mM NaCl, 0.4 mM EDTA, 4 mM DTT and 20% glycerol; pH6.5 buffer contains 20 mM HEPES pH6.5, 120 mM NaCl, 0.4 mM EDTA, 4 mM DTT and 20% glycerol, pH7.0 buffer contains 20 mM HEPES pH7.0, 120 mM NaCl, 0.4 mM EDTA, 4 mM DTT and 20% glycerol. Upon addition of 20 µM FRET substrate, the reaction progress was monitored for 1 hr. The first 15 min of reaction was used to calculate initial velocity (V_i) via linear regression in prism 5. Main protease displays highest proteolytic activity in pH6.5 buffer. All the following enzymatic assays were carried in pH6.5 buffer.

For the measurements of K_m/V_{max}, screening the protease inhibitor library, as well as IC_{50} measurements, proteolytic reaction with 100 nM Main protease in 100 µl pH6.5 reaction buffer was carried out at 30 °C in a Cytation 5 imaging reader (Thermo Fisher Scientific) with filters for excitation at 360/40 nm and emission at 460/40 nm. Reactions were monitored every 90 s. For

K_m/V_{max} measurements, a FRET substrate concentration ranging from 0 to 200 µM was applied. The initial velocity of the proteolytic activity was calculated by linear regression for the first 15 min of the kinetic progress curves. The initial velocity was plotted against the FRET concentration with the classic Michaelis-Menten equation in Prism 5 software. For the screening protease inhibitor library and IC_{50} measurements, 100 nM Main protease was incubated with protease inhibitor at 30°C for 30 min in reaction buffer, and then the reaction was initiated by adding 10 µM FRET substrate, the reaction was monitored for 1 h, and the initial velocity was calculated for the first 15 min by linear regression. The IC_{50} was calculated by plotting the initial velocity against various concentrations of protease inhibitors by use of a dose-response curve in Prism 5 software. Proteolytic reaction progress curve kinetics measurements with GC376, MG132, Boceprevir, Calpain inhibitor II, and Calpain inhibitor XII used for curve fitting, were carried out as follows: 5 nM Main protease protein was added to 20 µM FRET substrate with various concentrations of testing inhibitor in 200 µl of reaction buffer at 30 °C to initiate the proteolytic reaction. The reaction was monitored for 4 hrs. The progress curves were fit to a slow binding Morrison equation (equation 3) as described previously [15,35]:

$$E + I \underset{k_{-1}}{\overset{k_1}{\leftrightarrow}} EI \underset{k_{-2}}{\overset{k_2}{\leftrightarrow}} EI* \qquad (1)$$

$$K_I = k_{-1}/k_1 \qquad (2)$$

$$P(t) = P_0 + V_s t - (Vs - V_0)(1 - e^{-kt})/k \qquad (3)$$

$$k = k_2[I]/(K_I + [I]) \qquad (4)$$

where P(t) is the fluorescence signal at time t, P_0 is the background signal at time zero, V_0, V_s, and and k represent, respectively, the initial velocity, the final steady-state velocity and the apparent first-order rate constant for the establishment of the equilibrium between EI and EI* [35].

k_2/K_I is commonly used to evaluate the efficacy for covalent inhibitor. We observed substrate depletion when proteolytic reactions progress longer than 90 min, therefore only first 90 min of the progress curves were used in the curve fitting (Figure 6 middle column). In this study, we could not accurately determine the k_2 for the protease inhibitors: Calpain inhibitor II, MG132, Boceprevir, and Calpain inhibitor XII, due to the very slow k_2 in these case: significant substrate depletion before the establishment of the equilibrium between EI and EI*. In these cases, K_I was determined with Morrison equation in Prism 5.

Differential scanning fluorimetry (DSF). The binding of protease inhibitors on Main protease protein was monitored by differential scanning fluorimetry (DSF) using a Thermal Fisher QuantStudio™ 5 Real-Time PCR System. TSA plates were prepared by mixing Main protease protein (final concentration of 3 μM) with inhibitors, and incubated at 30 °C for 30 min. 1× SYPRO orange (Thermal Fisher) were added and the fluorescence of the plates were taken under a temperature gradient ranging from 20 to 90 °C (incremental steps of 0.05 °C/s). The melting temperature (T_m) was calculated as the mid-log of the transition phase from the native to the denatured protein using a Boltzmann model (Protein Thermal Shift Software v1.3). Thermal shift which was represented as ΔT_m was calculated by subtracting reference melting temperature of proteins in DMSO from the T_m in the presence of compound.

Cytotoxicity measurement. A549, MDCK, HCT-8, Caco-2, Vero, and BEAS2B cells for cytotoxicity CPE assays were seeded and grown overnight at 37 °C in a 5% CO2 atmosphere to ~90% confluence on the next day. Cells were washed with PBS buffer and 200 μl DMEM with 2% FBS and 1% penicillin−streptomycin, and various concentration of protease inhibitors was added to each well. 48 hrs after addition the protease inhibitors, cells were stained with 66 μg/ mL neutral red for 2 h, and neutral red uptake was measured at an absorbance at 540 nm using a

Multiskan FC microplate photometer (Thermo Fisher Scientific). The CC_{50} values were calculated from best-fit dose−response curves using GraphPad Prism 5 software.

SARS-CoV-2 CPE assay. Antiviral activities of test compounds were determined in nearly confluent cultures of Vero 76 cells. The assays were performed in 96-well Corning microplates. Cells were infected with approximately 60 cell culture infectious doses ($CCID_{50}$) of SARS-CoV-2 and 50% effective concentrations (EC_{50}) were calculated based on virus-induced cytopathic effects (CPE) quantified by neutral red dye uptake after 5 days of incubation. Three microwells at each concentration of compound were infected. Two uninfected microwells served as toxicity controls. Cells were stained for viability for 2 h with neutral red (0.11% final concentration). Excess dye was rinsed from the cells with phosphate-buffered saline (PBS). The absorbed dye was eluted from the cells with 0.1 ml of 50% Sörensen's citrate buffer (pH 4.2)-50% ethanol. Plates were read for optical density determination at 540 nm. Readings were converted to the percentage of the results for the uninfected control using an Excel spreadsheet developed for this purpose. EC_{50} values were determined by plotting percent CPE versus $\log_{10}$ inhibitor concentration. Toxicity at each concentration was determined in uninfected wells in the same microplates by measuring dye uptake.

SARS-CoV-2 VYR assay. Virus yield reduction (VYR) assays were conducted by first replicating the viruses in the presence of test compound. Supernatant was harvested 3 days post-infection from each concentration of test compound and the virus yield was determined by endpoint dilution method. Briefly, supernatant virus was serially diluted in $\log_{10}$ increments then plated onto quadruplicate wells of 96-well plates seeded with Vero 76 cells. The presence or absence of CPE for determining a viral endpoint was evaluated by microscopic examination of

cells 6 days after infection. From these data, 90% virus inhibitory concentrations (EC_{90}) were determined by regression analysis.

Influenza A virus A/California/07/2009 (H1N1) plaque reduction assay. The plaque assay was performed according to previously published procedures.[36]

Acknowledgements

This research was partially supported by the National Institutes of Health (NIH) (Grant AI147325) and the Arizona Biomedical Research Centre Young Investigator grant (ADHS18-198859) to J. W. B. H. and B. T. thanks for the support from the Respiratory Diseases Branch, National Institute of Allergy and Infectious Diseases, NIH, USA (Contract N01-AI-30048).

Author contributions

J. W. and C. M. conceived and designed the study. C. M. expressed the M^{pro} with the assistance of T. S. C.M. performed the primary screening, secondary IC_{50} determination, thermal shift-binding assay, and enzymatic kinetic studies. B. H. and B. T performed the SARS-CoV-2 CPE and VYR assay. Y. H. performed the plaque reduction assay with influenza A/California/07/2009 (H1N1) virus. J. W. secured funding and supervised the study. J. W. and C. M. wrote the manuscript with the input from others.

Competing interests

J. W. and C. M. are inventors of a pending patent that claims the use of the identified compounds for COVID-19.

References

1 https://www.who.int/emergencies/diseases/novel-coronavirus-2019.

2 Mahase, E. Coronavirus: covid-19 has killed more people than SARS and MERS combined, despite lower case fatality rate. *BMJ* **368**, m641, doi:10.1136/bmj.m641 (2020).

3 Lu, R. *et al.* Genomic characterisation and epidemiology of 2019 novel coronavirus: implications for virus origins and receptor binding. *Lancet* **395**, 565-574, doi:10.1016/S0140-6736(20)30251-8 (2020).

4 Wu, A. *et al.* Genome Composition and Divergence of the Novel Coronavirus (2019-nCoV) Originating in China. *Cell Host Microbe* **27**, 325-328, doi:10.1016/j.chom.2020.02.001 (2020).

5 Gorbalenya, A. E. *et al.* The species Severe acute respiratory syndrome-related coronavirus: classifying 2019-nCoV and naming it SARS-CoV-2. *Nat. Microbiol.* doi:10.1038/s41564-020-0695-z (2020).

6 Tang, B. *et al.* An updated estimation of the risk of transmission of the novel coronavirus (2019-nCov). *Infect. Dis. Model.* **5**, 248-255, doi:https://doi.org/10.1016/j.idm.2020.02.001 (2020).

7 Zhang, L. *et al.* Crystal structure of SARS-CoV-2 main protease provides a basis for design of improved alpha-ketoamide inhibitors. *Science*, doi:10.1126/science.abb3405 (2020).

8 Anand, K., Ziebuhr, J., Wadhwani, P., Mesters, J. R. & Hilgenfeld, R. Coronavirus main proteinase (3CLpro) structure: basis for design of anti-SARS drugs. *Science* **300**, 1763-1767, doi:10.1126/science.1085658 (2003).

9 Jin, Z. *et al.* Structure of M(pro) from COVID-19 virus and discovery of its inhibitors. *Nature*, doi:10.1038/s41586-020-2223-y (2020).

10 Pedersen, N. C. *et al.* Efficacy of a 3C-like protease inhibitor in treating various forms of acquired feline infectious peritonitis. *J Feline Med Surg* **20**, 378-392, doi:10.1177/1098612X17729626 (2018).

11 Kim, Y. *et al.* Reversal of the Progression of Fatal Coronavirus Infection in Cats by a Broad-Spectrum Coronavirus Protease Inhibitor. *PLoS Pathog* **12**, e1005531, doi:10.1371/journal.ppat.1005531 (2016).

12 Kim, Y. *et al.* Broad-spectrum antivirals against 3C or 3C-like proteases of picornaviruses, noroviruses, and coronaviruses. *J. Virol.* **86**, 11754-11762, doi:10.1128/JVI.01348-12 (2012).

13 Hayden, F. G. *et al.* Phase II, randomized, double-blind, placebo-controlled studies of ruprintrivir nasal spray 2-percent suspension for prevention and treatment of experimentally induced rhinovirus colds in healthy volunteers. *Antimicrob. Agents Chemother*. **47**, 3907-3916, doi:10.1128/aac.47.12.3907-3916.2003 (2003).

14 Shie, J. J. *et al.* Inhibition of the severe acute respiratory syndrome 3CL protease by peptidomimetic alpha,beta-unsaturated esters. *Bioorg. Med. Chem.* **13**, 5240-5252, doi:10.1016/j.bmc.2005.05.065 (2005).

15 Musharrafieh, R. *et al.* Validating Enterovirus D68-2A(pro) as an Antiviral Drug Target and the Discovery of Telaprevir as a Potent D68-2A(pro) Inhibitor. *J. Virol.* **93**, doi:10.1128/JVI.02221-18 (2019).

16 Kuo, C.-J. *et al.* Design, synthesis, and evaluation of 3C protease inhibitors as anti-enterovirus 71 agents. *Bioorg. Med. Chem.* **16**, 7388-7398, doi:https://doi.org/10.1016/j.bmc.2008.06.015 (2008).

17 Bonuccelli, G. *et al.* Proteasome inhibitor (MG-132) treatment of mdx mice rescues the expression and membrane localization of dystrophin and dystrophin-associated proteins. *Am J Pathol* **163**, 1663-1675, doi:10.1016/S0002-9440(10)63523-7 (2003).

18 Mani, S. K. *et al.* In vivo administration of calpeptin attenuates calpain activation and cardiomyocyte loss in pressure-overloaded feline myocardium. *Am J Physiol Heart Circ Physiol* **295**, H314-326, doi:10.1152/ajpheart.00085.2008 (2008).

19 Peng, S., Kuang, Z., Zhang, Y., Xu, H. & Cheng, Q. The protective effects and potential mechanism of Calpain inhibitor Calpeptin against focal cerebral ischemia-reperfusion injury in rats. *Mol Biol Rep* **38**, 905-912, doi:10.1007/s11033-010-0183-2 (2011).

20 Akdemir, O. *et al.* Therapeutic efficacy of SJA6017, a calpain inhibitor, in rat spinal cord injury. *J Clin Neurosci* **15**, 1130-1136, doi:10.1016/j.jocn.2007.08.011 (2008).

21 Li, S. Z. *et al.* ALLN hinders HCT116 tumor growth through Bax-dependent apoptosis. *Biochem Biophys Res Commun* **437**, 325-330, doi:10.1016/j.bbrc.2013.06.088 (2013).

22 Delli Pizzi, S. *et al.* Morphological and metabolic changes in the nigro-striatal pathway of synthetic proteasome inhibitor (PSI)-treated rats: a MRI and MRS study. *PLoS One* **8**, e56501, doi:10.1371/journal.pone.0056501 (2013).

23 Wang, M. *et al.* Remdesivir and chloroquine effectively inhibit the recently emerged novel coronavirus (2019-nCoV) in vitro. *Cell Res* **30**, 269-271, doi:10.1038/s41422-020-0282-0 (2020).

24 Li, G. & De Clercq, E. Therapeutic options for the 2019 novel coronavirus (2019-nCoV). *Nat Rev Drug Discov* **19**, 149-150, doi:10.1038/d41573-020-00016-0 (2020).

25 Grein, J. *et al.* Compassionate Use of Remdesivir for Patients with Severe Covid-19. *N. E. J. Med.* doi:10.1056/NEJMoa2007016 (2020).

26 Holshue, M. L. *et al.* First Case of 2019 Novel Coronavirus in the United States. *N Engl J Med* **382**, 929-936, doi:10.1056/NEJMoa2001191 (2020).

27 Cao, B. *et al.* A Trial of Lopinavir–Ritonavir in Adults Hospitalized with Severe Covid-19. *N. E. J. Med.* doi:10.1056/NEJMoa2001282 (2020).

28 Zumla, A., Chan, J. F., Azhar, E. I., Hui, D. S. & Yuen, K. Y. Coronaviruses - drug discovery and therapeutic options. *Nat. Rev. Drug Discov.* **15**, 327-347, doi:10.1038/nrd.2015.37 (2016).

29 Ono, Y., Saido, T. C. & Sorimachi, H. Calpain research for drug discovery: challenges and potential. *Nat. Rev. Drug Discov.* **15**, 854-876, doi:10.1038/nrd.2016.212 (2016).

30 Xue, X. *et al.* Structures of two coronavirus main proteases: implications for substrate binding and antiviral drug design. *J. Virol.* **82**, 2515-2527, doi:10.1128/JVI.02114-07 (2008).

31 Hoffmann, M. *et al.* SARS-CoV-2 Cell Entry Depends on ACE2 and TMPRSS2 and Is Blocked by a Clinically Proven Protease Inhibitor. *Cell*, doi:https://doi.org/10.1016/j.cell.2020.02.052 (2020).

32 Shang, L. *et al.* Biochemical characterization of recombinant Enterovirus 71 3C protease with fluorogenic model peptide substrates and development of a biochemical assay. *Antimicrob Agents Chemother* **59**, 1827-1836, doi:10.1128/AAC.04698-14 (2015).

33 Cai, Q. *et al.* Conformational plasticity of the 2A proteinase from enterovirus 71. *J. Virol.* **87**, 7348-7356, doi:10.1128/JVI.03541-12 (2013).

34 Cady, S. D., Wang, J., Wu, Y., DeGrado, W. F. & Hong, M. Specific binding of adamantane drugs and direction of their polar amines in the pore of the influenza M2 transmembrane domain in lipid bilayers and dodecylphosphocholine micelles determined by NMR spectroscopy. *J. Am. Chem. Soc.* **133**, 4274-4284, doi:10.1021/ja102581n (2011).

35 Morrison, J. F. & Walsh, C. T. The behavior and significance of slow-binding enzyme inhibitors. *Adv Enzymol Relat Areas Mol Biol* **61**, 201-301, doi:10.1002/9780470123072.ch5 (1988).

36 Ma, C., Zhang, J. & Wang, J. Pharmacological Characterization of the Spectrum of Antiviral Activity and Genetic Barrier to Drug Resistance of M2-S31N Channel Blockers. *Mol Pharmacol* **90**, 188-198, doi:10.1124/mol.116.105346 (2016).